Supporting information

to

Photoinduced damage of AsLOV2 domain is accompanied by increased singlet oxygen production due to flavin dissociation

Martina Petrenčáková, František Filandr, Andrej Hovan, Ghazaleh Yassaghi, Petr Man, Tibor Kožár, Marc-Simon Schwer, Daniel Jancura, Andreas Plückthun, Petr Novák, Pavol Miškovský, Gregor Bánó and Erik Sedlák

Predominant localization of singlet oxygen outside the protein

Singlet oxygen produced inside the protein matrix diffuses to the surrounding water environment. An upper limit for the effective diffusion time of $^1O_2$ escaping from the protein interior to water can be obtained using the analytical formula derived by Hovan et al. [Hovan et al. 2018]. Choosing reasonable limits for the $^1O_2$ partition coefficient in the protein/water environment, K_Δ<10, and for the diffusion constant of $^1O_2$ inside of the protein, D_Δ^{prot}>1.10^{-10} cm^{2}s^{-1} [Lepeshkevich et al. 2014], an upper estimate for the effective diffusion time, τ_Δ^{eff}<9 ns, was obtained for AsLOV2. This value is in good agreement with the estimated transient times reported for miniSOG and SOPP (3-60 ns) [Westberg et al. 2017]. The obtained escape-time was compared with the lifetime of $^1O_2$ in the protein interior environment, which was estimated using the method suggested by Lepeshkevich et al. [2014] for globular proteins. The size of AsLOV2 and the rate constants for $^1O_2$ deactivation by the individual amino acids (mostly Tyr, Trp, His, Met and Cys [Lindig et al. 1981, Michaeli et al.1994, Lepeshkevich et al. 2014]) were taken into account. The rate of $^1O_2$ deactivation by FMN was estimated on the basis of data with free riboflavin [Wilkinson et al. 1995]. This way the lifetime of $^1O_2$ was estimated to be τ_Δ^{LOV2}~400 ns for the AsLOV2 interior. This lifetime is significantly longer than the estimated escape-time. We therefore conclude that $^1O_2$ produced in AsLOV2 spends most of its lifetime in an aqueous environment, which is in accordance with the assumption used by Westberg et al. [2017].

References

Hovan, A. *et al.* Phosphorescence Kinetics of Singlet Oxygen Produced by Photosensitization in Spherical Nanoparticles. Part I. Theory. *The journal of physical chemistry. B* **122**, 5147-5153, doi:10.1021/acs.jpcb.8b00658 (2018).

Lepeshkevich, S. V. *et al.* Photosensitized singlet oxygen luminescence from the protein matrix of Zn-substituted myoglobin. *The journal of physical chemistry. A* **118**, 1864-1878, doi:10.1021/jp501615h (2014).

Lindig, B. A. & Rodgers, M. A. J. Rate Parameters for the Quenching of Singlet Oxygen by Water-Soluble and Lipid-Soluble Substrates in Aqueous and Micellar Systems. *Photochemistry and Photobiology* **33**, 627-634, doi:DOI 10.1111/j.1751-1097.1981.tb05468.x (1981).

Michaeli, A. & Feitelson, J. Reactivity of singlet oxygen toward amino acids and peptides. *Photochem Photobiol* **59**, 284-289, doi:10.1111/j.1751-1097.1994.tb05035.x (1994).

Westberg, M., Bregnhoj, M., Etzerodt, M. & Ogilby, P. R. No Photon Wasted: An Efficient and Selective Singlet Oxygen Photosensitizing Protein. *The journal of physical chemistry. B* **121**, 9366-9371, doi:10.1021/acs.jpcb.7b07831 (2017).

Wilkinson, F., Helman, W. P. & Ross, A. B. Rate Constants for the Decay and Reactions of the Lowest Electronically Excited Singlet-State of Molecular-Oxygen in Solution - an Expanded and Revised Compilation. *Journal of Physical and Chemical Reference Data* **24**, 663-1021, doi:Doi 10.1063/1.555965 (1995).

Figure S1

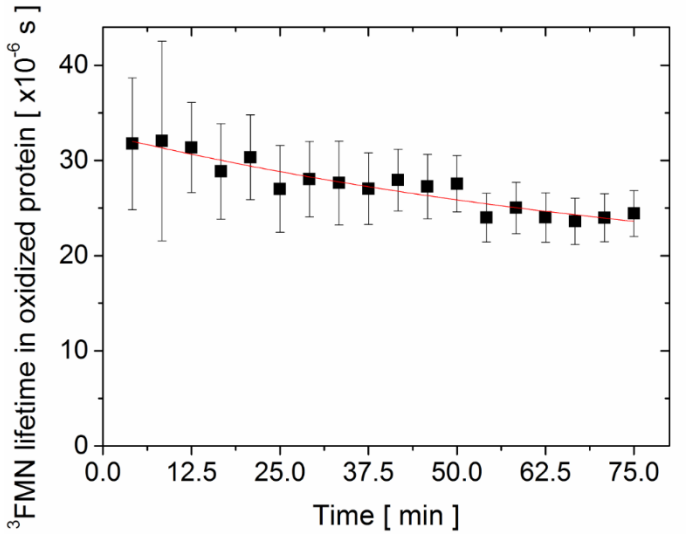

Figure S1. The values of τ_T^{prot*} as a function of the irradiation time obtained from fitting transient absorption signals of AsLOV2 C450A. The errors represent 3 times the standard deviation of the fitting parameter.

Analysis of the model of the irradiation-induced degradation of AsLOV2 C450A

The set of coupled differential equations describing the concentration of FMN in C450A, C450A* and in the water environment (before bleaching) can be written as follows:

$$\frac{d[\text{FMN}]_{\text{prot}}}{dt} = -k_1[\text{FMN}]_{\text{prot}}$$

$$\frac{d[\text{FMN}]_{\text{prot*}}}{dt} = k_1[\text{FMN}]_{\text{prot}} - k_2[\text{FMN}]_{\text{prot*}}$$

$$\frac{d[\text{FMN}]_{\text{water}}}{dt} = k_2[\text{FMN}]_{\text{prot*}} - k_3[\text{FMN}]_{\text{water}}$$

The analytical solutions of these equations are:

$$[\text{FMN}]_{\text{prot}} = [\text{FMN}]^0_{\text{prot}}\, e^{-k_1 t} \qquad \text{....(Eq. S1)}$$

$$[\text{FMN}]_{\text{prot*}} = \frac{k_1[\text{FMN}]^0_{\text{prot}}}{k_1 - k_2}\left(e^{-k_2 t} - e^{-k_1 t}\right)$$

....(Eq. S2)

$$[\text{FMN}]_{\text{water}} = \frac{k_1 k_2[\text{FMN}]^0_{\text{prot}}}{k_1 - k_2}\left(\frac{e^{-k_2 t} - e^{-k_3 t}}{k_3 - k_2} - \frac{e^{-k_1 t} - e^{-k_3 t}}{k_3 - k_1}\right)$$

....(Eq. S3)

Analysis of the model of the irradiation-induced degradation of AsLOV2 wt

The observed kinetics of Abs_{prot} and Abs_{water} were analyzed in a semi-empirical way, assuming a linear decrease of the $[FMN_{prot}]$ concentration in the studied time range. This assumption is consistent with a constant source term of FMN in water, assigned as K:

$$\frac{d[\mathrm{FMN}]_{\mathrm{water}}}{dt} = K - k_3[\mathrm{FMN}]_{\mathrm{water}}$$

The solution gives the time-dependence of the FMN concentration in water:

$$[\mathrm{FMN}]_{\mathrm{water}} = \frac{K}{k_3}(1 - e^{-k_3 t})$$

This function was used to fit the Abs_{water} values (black squares) in the Figure 3A, using the same rate of FMN bleaching k_3 as for the mutant (determined in the auxiliary bleaching experiment). It can be seen that the shape of the curve is well described by the bleaching effect.

References

Westberg, M., Bregnhoj, M., Etzerodt, M. & Ogilby, P. R. Temperature Sensitive Singlet Oxygen Photosensitization by LOV-Derived Fluorescent Flavoproteins. *The journal of physical chemistry. B* **121**, 2561-2574, doi:10.1021/acs.jpcb.7b00561 (2017).

Torra, J. *et al.* Tailing miniSOG: structural bases of the complex photophysics of a flavin-binding singlet oxygen photosensitizing protein. *Sci Rep* **9**, 2428, doi:10.1038/s41598-019-38955-3 (2019).

Figure S2

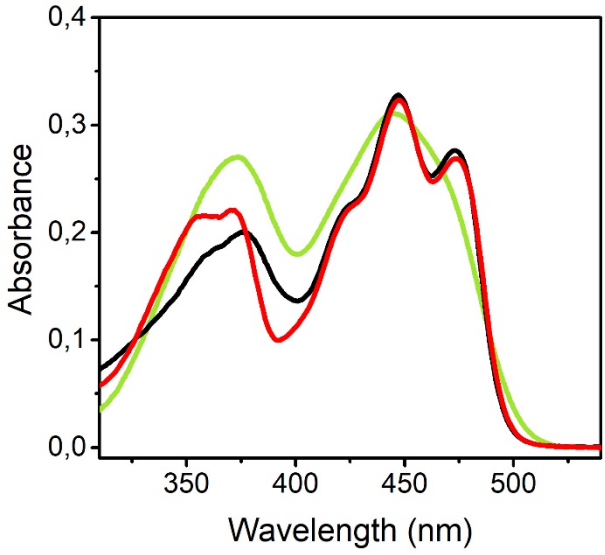

Figure S2. Absorption spectra of AsLOV2 wt (**black**), AsLOV2-C450A (**red**), and free FMN (**green**) at 25 μM concentration.

Figure S3

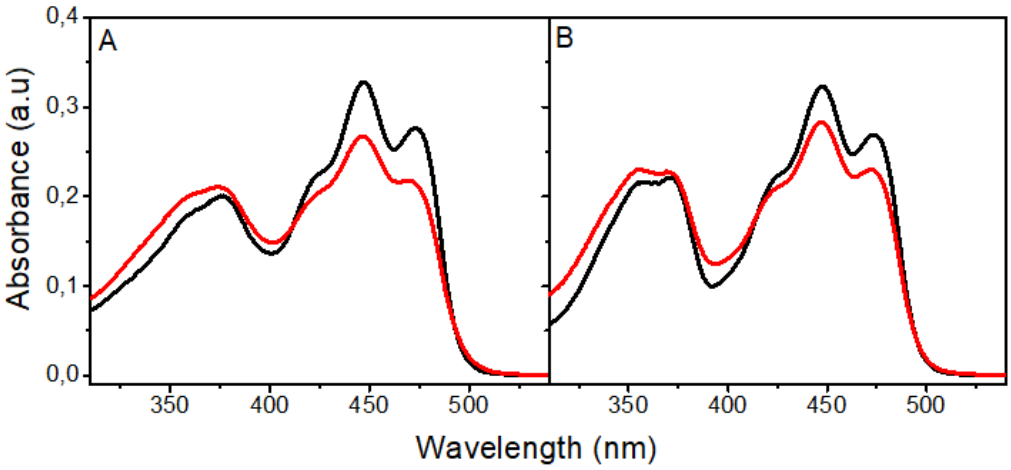

Figure S3. Absorption spectra of AsLOV2 wt (A) and AsLOV2 C450A (B) before (**black**) and after (**red**) illumination. Proteins concentration was 25 µM.

Figure S4

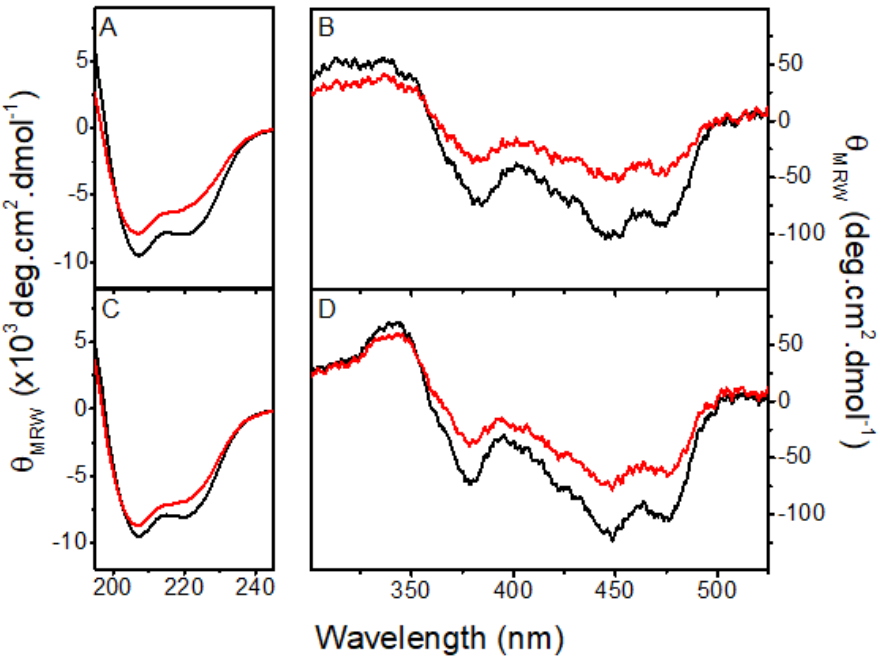

Figure S4. Circular dichroism spectra of AsLOV2 wt (A, B) and AsLOV2 C450A (C, D) in the far-UV (A, C) and the near-UV and visible regions (B, D) before (**black**) and after (**red**) illumination.

Figure S5

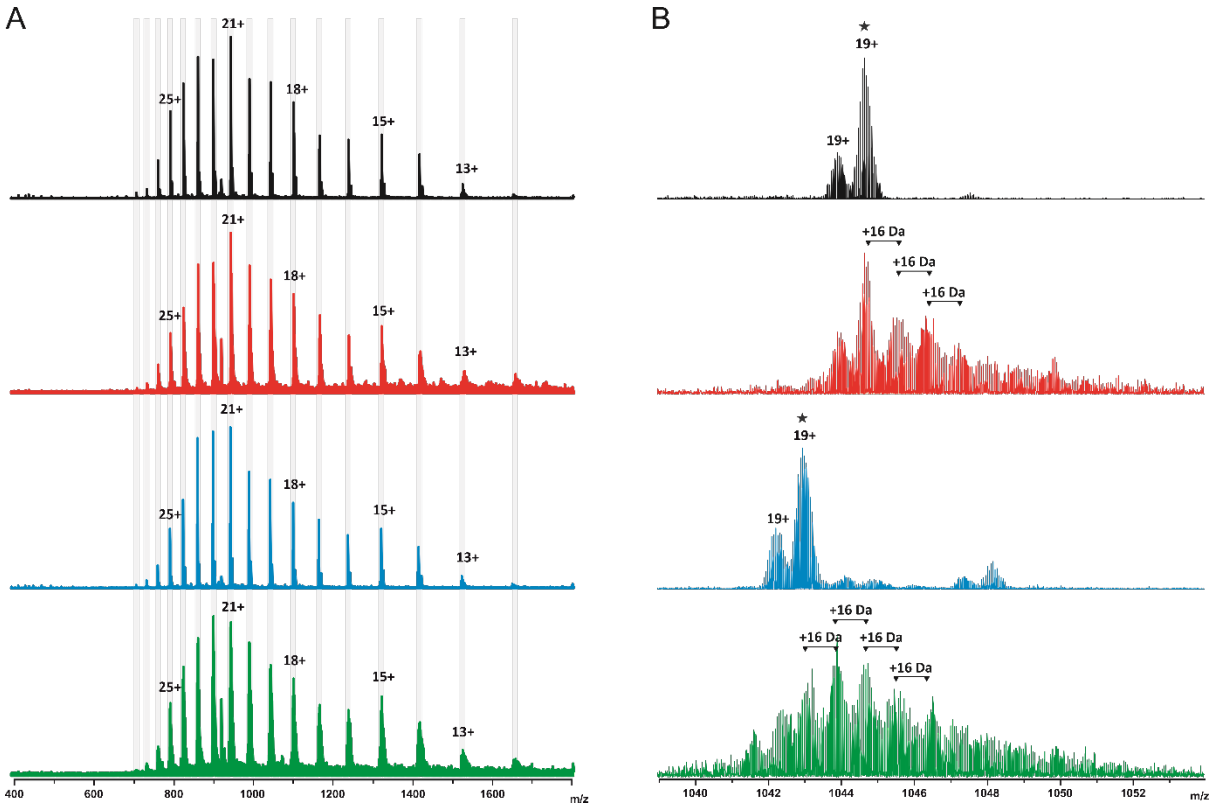

Figure S5. Analysis of intact proteins by nESI-FT-ICR MS. **A** – from top to bottom - broad band spectra of wild-type AsLOV2 before (**black**) and after (**red**) irradiation and of C450A form before (**blue**) and after (**green**) irradiation. Clean spectra in panel **A** show classical ESI protein charge state envelope with no signals of peptides/fragments. Panel **B** with zoom on the charge state 19+ demonstrates much higher modification extent in the C450A variant than in the wild-type AsLOV2. Peaks marked with a star symbol are methylated forms of protein.

Figure S6

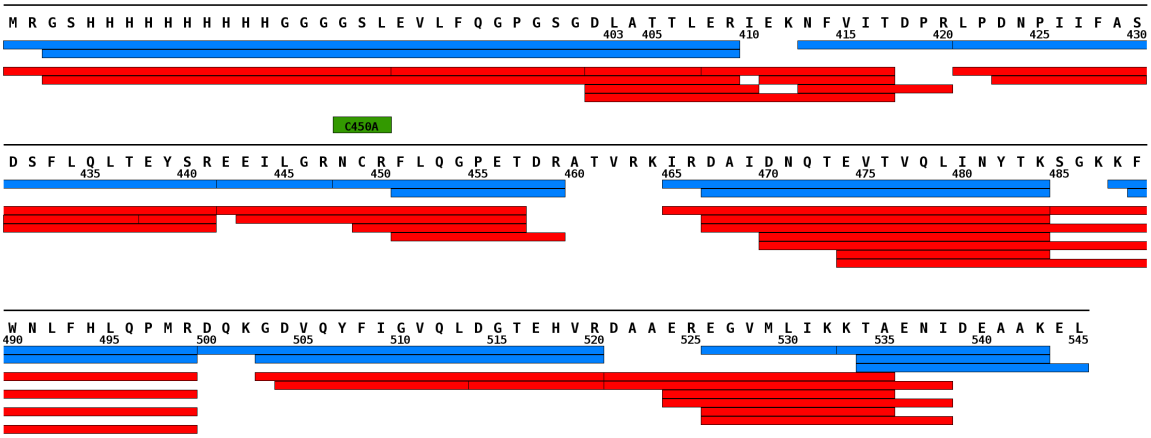

Figure S6. Sequence coverage of AsLOV2 obtained in bottom-up experiments. Proteins were digested by trypsin (**blue**) or Asp-N (**red**), analyzed by LC-MS/MS and the data were searched by MASCOT and PEAKS algorithms. Identified peptides are shown as individual bars. The position of **Cys450** is highlighted above the sequence. Sequence coverage for both proteases was 91% and combined coverage is 97%.

Figure S7

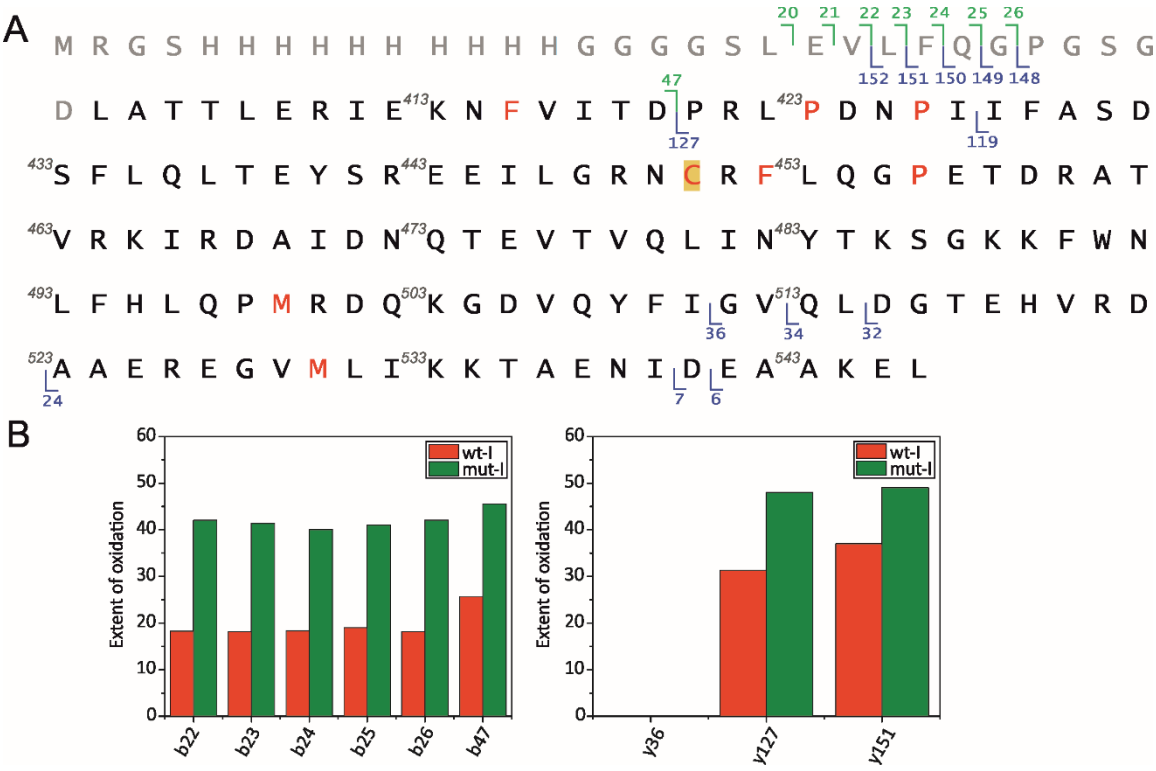

Figure S7. A - AsLOV2 sequence with fragments (b- and y-type ions shown in green and blue, respectively) observed in the top-down MS/MS experiment depicted by black check marks. The site of the C450A mutation is colored in yellow. The His-tag sequence is not numbered and is shown in grey, the native sequence starts with Leu404. Red color highlights residues that were observed in bottom-up as significantly different between the irradiated wt and mut (C450A) form. B - Bar graphs showing quantification of blue-light induced oxidation at selected sites (fragment ions) in both protein forms – wt in red and C450A in green.

Figure S8

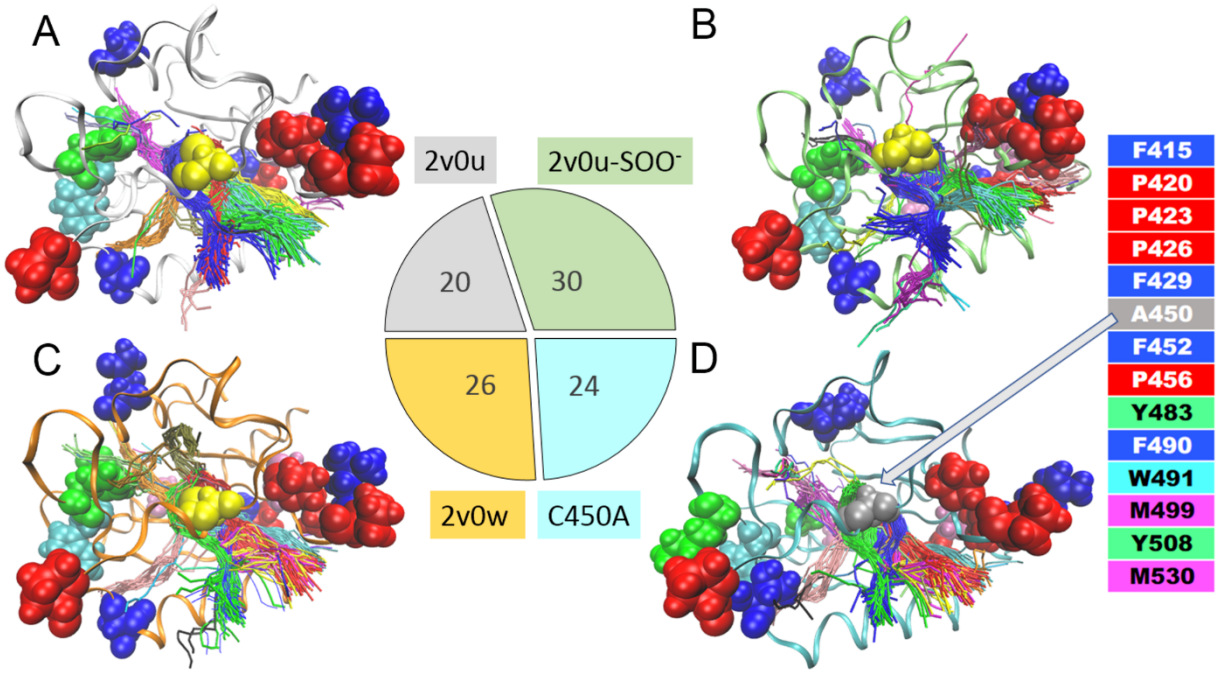

Figure S8. VMD visualization (https://www.ks.uiuc.edu/Research/vmd/) Caver-calculated tunnels resulting from 5ns MD simulations (coordinates saved at 10 ps intervals) of different AsLOV2-related and modified proteins. The color-coded amino acids shown in CPK representation correspond to the amino acids summarized in Figure 6. The C450 atoms are colored yellow; the A450 atoms are in grey. The starting points of all clusters correspond to these amino acids. The color coding of the tunnels represented as sticks do not correspond to the color coding of the amino acids, but are for their distinction only. The backbone of the proteins is shown in ribbon representation. The tunnels were calculated for all 500 saved protein conformations and subsequently clustered with the Caver program. The central pie chart shows the number of clusters for each protein simulated. The tunnels coloring (the tunnels are shown as connected sticks) is arbitrary and do not match the amino acid coloring in the proximity of the tunnels. **A)** simulation based on PDB ID: 2v0u structure. **B)** simulation with *in silico* -SOO^- -modified C450 (PDB ID: 2v0u). **C)** PDB ID: 2v0w with chemical bond between C450 and FMN (FMN not shown on the figure). **D)** simulation of 2u0v-C450A mutant of AsLOV2.

Figure S9

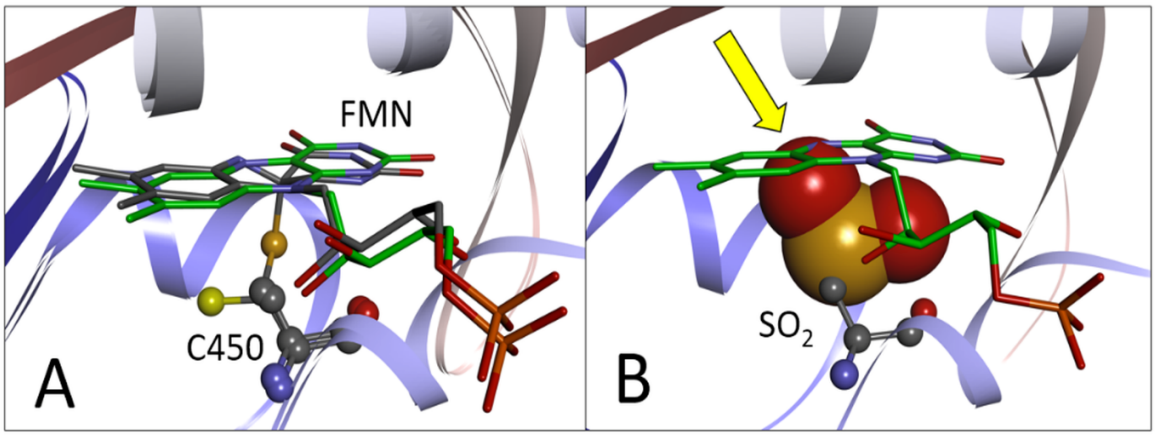

Figure S9. A) Superposition of PDB ID: 2w0u (FMN with green carbons) and PDB ID: 2v0w (FMN bound to Cys450 with grey-colored carbons). **B)** -SH to -SO_2^- substitution in C450 with marked atomic clash of the generated structure.

Figure S10

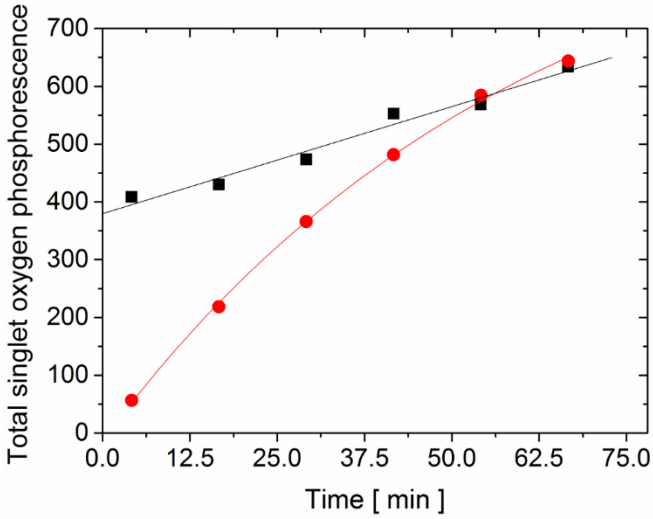

Figure S10. The total (integrated) $^1O_2$ phosphorescence signal produced by AsLOV2 C450A (black squares) and AsLOV2 wt (red circles) as a function of the irradiation time. Please note that the production of $^1O_2$ by AsLOV2 wt practically ends at 25 μs after the laser pulse (Figure 1B), while it lasts well after 40 μs in the case of AsLOV2 C450A (Figure 1A).